Virology 447 (2013) 1–8

Contents lists available at ScienceDirect

Virology

journal homepage: www.elsevier.com/locate/yviro

The multifaceted effect of PB1-F2 specific antibodies on influenza A virus infection

I. Košík [1], I. Krejnusová [1], M. Práznovská, G. Russ *

Institute of Virology, Slovak Academy of Sciences, Dúbravská cesta 9, 845 05 Bratislava, Slovak Republic

ARTICLE INFO

Article history:
Received 23 May 2013
Returned to author for revisions
15 June 2013
Accepted 20 August 2013
Available online 13 September 2013

Keywords:
PB1-F2
Immunogenicity
Humoral immunity
DNA vaccination
Influenza
Antibodies

ABSTRACT

PB1-F2 is a small influenza A virus (IAV) protein encoded by an alternative reading frame of the PB1 gene. During IAV infection, antibodies to PB1-F2 proteins are induced. To determine their function and contribution to virus infection, three distinct approaches were employed: passive transfer of anti-PB1-F2 MAbs and polyclonal antibodies, active immunization with PB1-F2 peptides and DNA vaccination with plasmids expressing various parts of PB1-F2. Mostly N-terminal specific antibodies were detected in polyclonal sera raised to complete PB1-F2. Passive and active immunization revealed that antibodies recognizing the N-terminal part of the PB1-F2 molecule have no remarkable effect on the course of IAV infection. Interestingly antibodies against the C-terminal region of PB1-F2, obtained by immunization with KLH-PB1-F2 C-terminal peptide or DNA immunization with pC-ter.PB1-F2 plasmid, partially protected mice against virus infection. To our knowledge, this is the first report demonstrating the biological relevance of humoral immunity against PB1-F2 protein *in vivo*.

Introduction

Influenza continues to be a major public health problem. The World Health Organization (WHO) estimates that in a typical year, 10–20% of the world's population is infected with influenza, resulting in 3–5 million severe illnesses and up to half a million deaths. During pandemics, the losses are even greater. Pandemic global outbreaks have caused severe illness with high mortality rates; the 1918 Spanish outbreak in particular killed at least 20 million people worldwide. Currently, the most efficient strategy for control of influenza is yearly vaccination (Morens et al., 2010; Stohr, 2003; Taubenberger and Morens, 2006).

The flu is caused by the influenza virus which is a segmented, enveloped, and negative strand RNA virus. The genome of influenza virus consists of eight separate RNA segments that code for viral proteins: two envelope glycoproteins-hemagglutinin (HA) and neuraminidase (NA), matrix protein (M1), an ion channel protein (M2), nucleoprotein (NP), three proteins of polymerase complex (PB1, PB2 and PA), non-structural proteins NS1 and nuclear export protein (NEP/NS2), until recently considered to be non-structural protein (Muramoto et al., 2013; Shi et al., 2012). While searching for alternative reading frame peptides encoded by influenza A viruses (IAV) that are recognized by CD8+T cells, a PB1-F2 protein encoded by the (+1) ORF in PB1 gene was discovered (Chen et al., 2001). PB1-F2 is also a nonstructural protein. A third PB1-related protein translated from PB1, N40, has recently been identified. In addition to its mode of translation, PB1-F2 has several unique features. These include its absence from some IAV isolates (Zell et al., 2007), variable expression in the individual infected cells, rapid degradation, mitochondrial localization, formation of a nonselective ion channel (Henkel et al., 2010; Chen et al., 2001; Yamada et al., 2004), and apoptotic or pro-apoptotic properties. Further studies using mouse models support a role for PB1-F2 in pathogenicity and lethality (Alymova et al., 2011; de Wit et al., 2008; McAuley et al., 2010b) probably by disrupting a function of alveolar macrophages (Coleman, 2007). IAVs knocked out for the expression of PB1-F2 were not attenuated in the replication in tissue culture, but their pathogenicity and lethality for mice was considerably reduced. Also, PB1-F2-knockout viruses were cleared from lungs more rapidly and induced earlier immune response to the infection (Zamarin et al., 2006) implying that PB1-F2 played a role in the suppression of immune response responsible for viral clearance. PB1-F2 enhances inflammation during the primary viral infection of mice and increases both the frequency and severity of secondary bacterial pneumonia (McAuley et al., 2007).

During IAV infections, Abs are generated to both structural (*HA, NA, NP, NS2, M1, M2*,) and non-structural protein (*NS1*). Only Abs to HA can efficiently neutralize virus infectivity. Antibodies to PB1-F2 protein are induced in response to influenza A virus infection (Krejnusova et al., 2009). We have shown that PB1-F2-specific Abs

* Corresponding author.
E-mail address: virugrus@savba.sk (G. Russ).
[1] Authors contributed equally.

0042-6822/$ - see front matter © 2013 Elsevier Inc. All rights reserved.
http://dx.doi.org/10.1016/j.virol.2013.08.022

could be detected via immunoprecipitation or immunofluorescence assays both in immune mouse and human convalescent sera. It has been reported that humans generate anti-PB1-F2 antibodies, as measured using a phage library expressing PB1-F2 sequences (Khurana et al., 2009). It is not known whether these antibodies can modulate the functional outcomes of PB1-F2 expression and course of disease. In the present study, we have used a number of assays for analysis of anti-PB1-F2 antibody responses, focusing on their effect on virus infection. We find that PB1-F2 specific antibodies directed against the C-terminal part of the molecule reasonably protect mice against IAV infection. On the other hand PB1-F2 specific antibodies which are directed predominantly to the N-terminal part of the molecule do not remarkably affect course of infection. Based on this analysis and the data presented in this study, it is clear that the biological relevance of anti-PB1-F2 specific antibodies in IAV infections is complex.

Results and discussion

"*In silico*" analysis predicts that PB1-F2 specific antibodies are most likely induced to the N-terminal part of PB1-F2 molecule.

Initially we applied "*in silico*" analysis for prediction of epitopes (B cell epitopes) recognized by PB1-F2 specific antibodies in immune sera. The complex prediction of beta-turns (Fig. 1A.1), accessibility (Fig. 1A.2), flexibility (Fig. 1A.3), hydrophilicity (Fig. 1A.4),antigenic propensity (Fig. 1A.6), was performed (December 2012http://tools.immuneepitope.org/tools/bcell/iedb_input). Although widely employed immunogenicity prediction algorithm (Kolaskar and Tongaonkar, 1990) (Fig. 1A.5) has predicted antibody binding sites even in the C-terminus, novel BepiPred method using a combination of a hidden Markov model and a propensity scale method determined a major antibody binding site in the N-terminus (Fig. 1A). Five out of six analyses predict antibody binding sites in N-terminal part of the PB1-F2, one in both N-terminal a C-terminal parts of the molecule and one mainly in the C-terminal part.

ELISA with peptides corresponding to various regions of PB1-F2 and immunofluorescence confirmed that N-terminal part of molecule is the major target for specific antibodies.

To validate the outcome of "*in silico*" analysis, PB1-F2 specific serum obtained by immunization of mice with purified PB1-F2-MBP protein was performed. As shown in Fig. 1B, typical serum contained antibodies recognizing in ELISA predominantly N-terminal peptide (3–13aa) and less efficiently also C-terminal peptide (65–87aa). According to "*in silico*" analysis, specific antibody binding sites should also be localized in region 14–41. Regrettably, no peptide(s) corresponding to this region was available. Accordingly, results of peptide ELISA correspond properly with "*in silico*"analysis. Interestingly, PB1-F2 specific MAb AG55 (Fig. 1C) bind only to N-terminal peptide (3–13). We are aware that direct binding of short peptides to the surface of plate partially or completely abolishes their conformation and mobility. Therefore PB1-F2 specific antibodies (recognizing conformational epitopes) could not be detected in such ELISA setting. To exclude direct binding, N-terminally biotinylated peptides derived from PB1-F2 ORF (7–16aa or 62–71aa) were attached to streptavidin pre-coated plate. Streptavidin pre-coated or direct coating of N terminally biotinylated peptides derived from PB1-F2 ORF (7–16aa or 62–71aa) was compared in its ability to interact with IMS anti PB1-F2-MBP (supplementary Fig. 1). Streptavidin pre-coating of wells and capture of PB1-F2 ORF derived peptides (7–16aa, 62–71aa) via biotin even worsened reactivity of all the screened anti PB1-F2-MBP sera. Employing of irrelevant IMS raised after MHV68 infection and irrelevant peptide derived from HA2 ORF (170–178aa) confirmed high specificity and relevance of used ELISA assay. In the experiments that followed we replaced peptide ELISA with indirect immunofluorescence of MDCK cells transiently transfected with pPB1-F2, pNter.PB1-F2, pCter.PB1-F2 and pPB1-F2 Stop 3aa, respectively. Similarly as in peptide ELISA PB1-F2 specific antibodies were detected in the immune sera raised against PB1-F2-MBP. Conformation is well preserved under these conditions. In immunofluorescence experiments the positive staining was detected only in transfected MDCK cells expressing either full length (pPB1-F2) or N-terminal part of PB1-F2 (pNter.PB1-F2) (Fig. 1D upper row). Interestingly, the staining pattern of MDCK cells expressing full length of PB1-F2 was apparently different from staining pattern corresponding to N-terminal part of PB1-F2. We assume that in MDCK cells full length PB1-F2 is localized in mitochondria, however N-terminal part PB1-F2 missing C-terminal mitochondrial localization signal is spread through cytosol and nucleus. Similarly nuclear localization of the PB1-F2 is typical for avian strain derived PB1-F2 (Chen et al., 2010; Kosik et al., 2013). We were unable to detect specific staining of MDCK cells expressing C-terminal part of PB1-F2. Although weak a clear signal was detected in ELISA for C-terminal peptide no staining of cells was seen in cells transfected by pCter.PB1-F2 following incubation with PB1-F2 specific serum obtained by immunization of mice with purified full length PB1-F2-MBP. We believe that this discrepancy can be explained by the higher sensitivity of ELISA as compared with indirect immunofluorescence of transfected cells. To confirm expression ability and transfection efficiency of the pPB1-F2, pNter.PB1-F2, pCter.PB1-F2 samples from the same transfection experiment were stained with PB1-F2 N terminally specific MAb (AG55) or PB1-F2-C terminally specific IMS anti PB1-F2 C_{73-87} –KLH respectively. As expected AG55 positive staining was only observed in the case of full length or N terminal part of the PB1-F2 (Fig. 1D middle row), while positive staining of transfected cells with IMS anti PB1-F2-C_{73-87} –KLH was only observed in the case of full length or C terminal part of the PB1-F2 (Fig. 1D below row). Neither IMSs nor MAb stained cells transfected by pPB1-F2 Stop3aa. To ensure no detectable expression of the PB1-F2 protein after transfection by pPB1-F2 Stop3aa western blot analysis was performed. It was not possible to detect PB1-F2 in cells transfected with pPB1-F2 Stop3aa or cells transfected with insert less plasmid pTriEx4 (Merck) neither with MAb AG55 nor IMS anti PB1-F2-MBP. Strong expression of the PB1-F2 protein was detected both MAb AG55 or IMS anti PB1-F2-MBP in the case of transfection with pPB1-F2 (supplementary Fig. 2). Based on the above presented results we suggest that PB1-F2 specific antibodies bind predominantly to the N-terminal part of the molecule.

Passive immunization with N-terminally specific MAbs has no remarkable effect on the course of infection.

To examine the effect of PB1-F2 specific antibody on virus infection, the mixture of two MAbs AG55 and LB66 was first passively transferred to a group of mice by intravenous rout and the mice were subsequently (within 2 h) challenged by PR8 (1LD50). For positive control, the group of mice were passively immunized with HA specific MAb H17L2, highly efficient in virus neutralization. In negative control the mice received HHV2 specific MAb 499. All MAbs used for passive immunization were of the same isotype. Survival rates and body weight changes were monitored daily. Virus in the lungs was determined by RCA on day 2, 6 and 10 days post infection. Two days post infection the similar titer of virus was detected in lungs of mice passively immunized with the mixture of N terminally PB1-F2 specific MAbs as in mice immunized with a negative control MAb or PBS respectively. As expected in the lungs of mice immunized H17L2 MAb there was almost no virus detected 2 days post infection. Six days post infection the virus in lungs was clearly detected only in mice immunized with negative control MAb and PBS. Ten days post infection, no virus was detected in the lungs of any groups of mice (Fig. 1A). Although weight loss was most remarkable in the

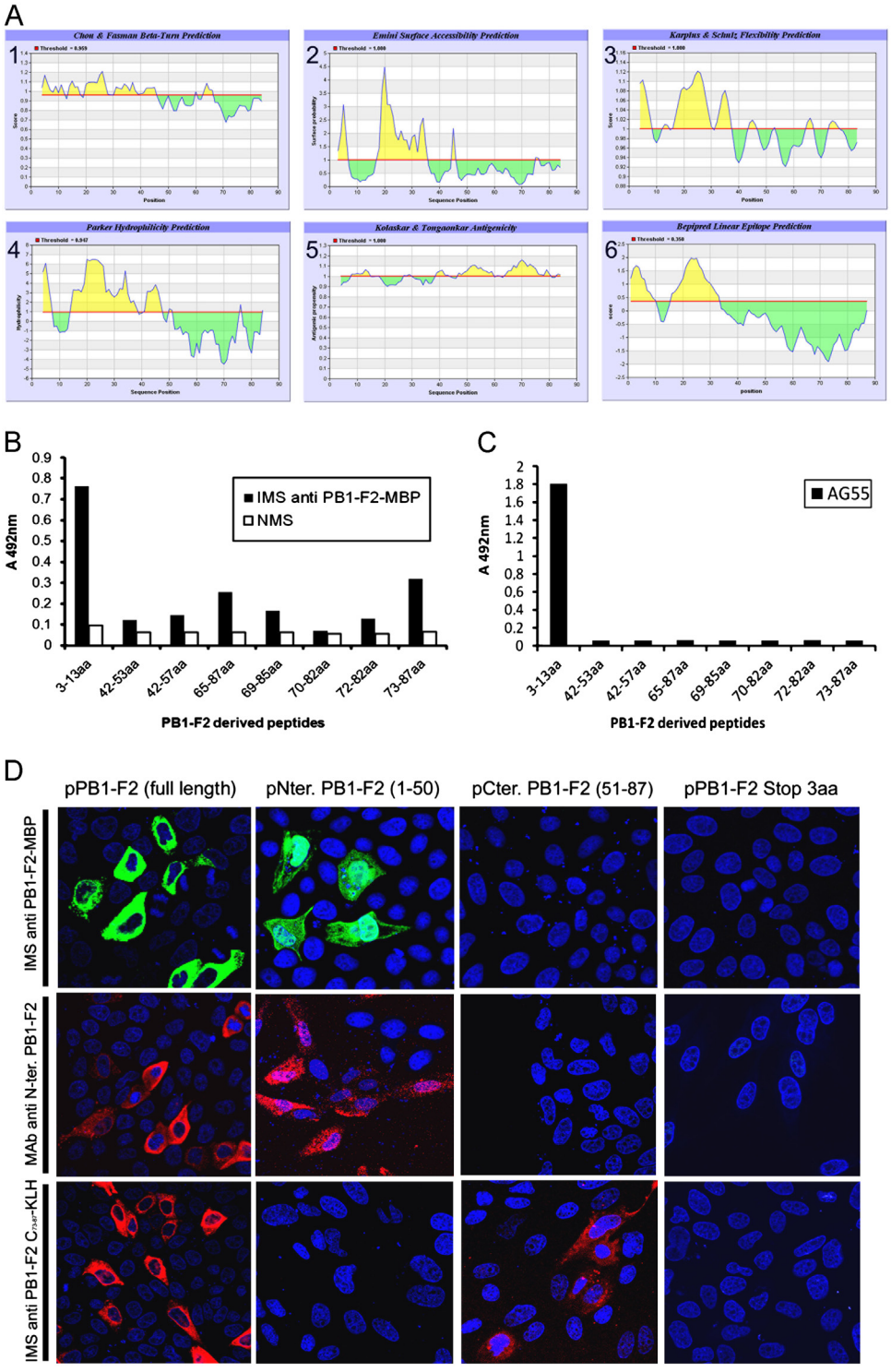

Fig. 1. *In silico* and *in vitro* analysis of immunogenic regions of PB1-F2 was performed. A complex web based tool for linear B cell epitopes prediction (http://tools.immuneepitope.org/tools/bcell) was employed to identify potential immunogenic sequential epitopes of PB1-F2. (A) Multiple parameters affecting immunogenicity were studied, including (A1) Beta-turn, (A2) surface accessibility, (A3) flexibility, (A4) hydrophilicity, two most recently used algorithms (A5) Kolaskar and Tongaonkar and (A6) Bepipred Linear Epitope Prediction of antigenicity prediction was also employed. (B) Eight PB1-F2 derived peptides were used to identify their interaction with antibobies presented in the polyclonal sera. Microtiter plates were coated by eight different PB1-F2 derived peptides (100 ng/well). Two hundred-fold diluted of IMSs raised after immunization with full length PB1-F2-MBP fusion protein were added to wells. Plate was washed and secondary HRP anti mouse and OPD substrate was subsequently incubated in the plate. Developed signal was measured by ELISA reader. All the samples were measured in triplicate. (C) The same procedure was performed with MAb AG55. (D) Abs recognizing conformational epitopes were evaluated in the serum raised to full length PB1-F2. Immunofluorescence was performed 24 h post transfection with plasmids expressing full length, N-terminal half, C-terminal half and Stop3aa mutant protein PB1-F2. Three slides were placed to each well of the six well plate and cells were added. At 60–70% confluence transfection mixtures was added and 24 later samples were fixed and permeabilized. Samples were individually incubated with 250-fold diluted IMS anti PB1-F2-MBP (upper row) and stained with 100-fold diluted goat anti mouse FITC conjugated secondary antibody (DAKO) or with undiluted hybridoma supernatant containing N terminally specific MAb AG55 (middle row) and stained with 100-fold diluted goat anti mouse Texas Red conjugated secondary antibody (Sigma-Aldrich) or with 50-fold diluted IMS anti $C_{73–87}$-KLH (lower row) and stained with 100-fold diluted goat anti mouse Texas Red secondary antibody (Sigma-Aldrich). After final washing samples and mounting with DAPI containing mounting medium (Santacruz Biotechnologies) samples were analyzed by confocal microscope Zeiss LSM 510 Meta.

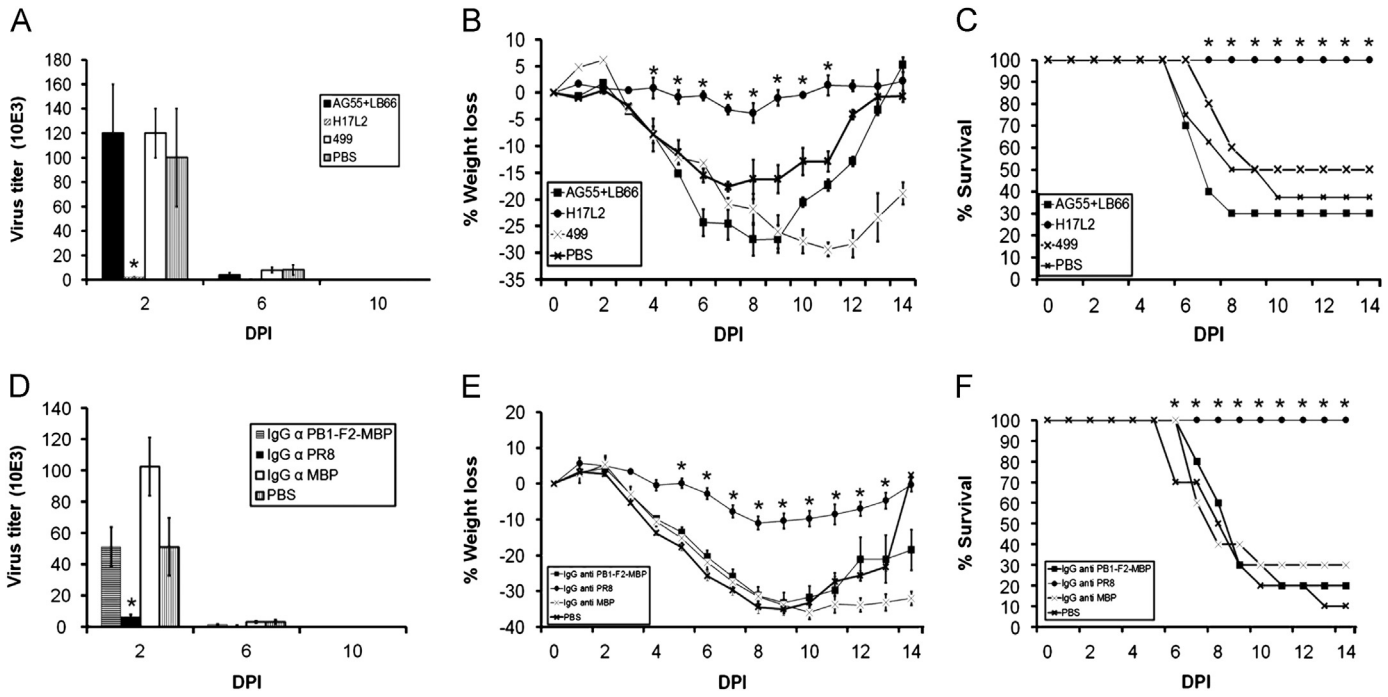

Fig. 2. Passive transfer of PB1-F2 specific MAbs and PAbs was used to determine the role of humoral immune response during the course of IAV infection. (A) In days post infection as indicated, two mice per group were sacrificed, lungs were homogenated in PBS and centrifuged in 4000 RPM for 10 min. Supernatant was used for RCA as described in materials and methods section. Duplicate samples were analyzed. Virus titer was determined as reciprocal of highest dilution producing positive staining of cells. (B) For severity of infection measurement of the body weight changes for individual mouse and (C) rate of survival was recorded and plotted. The same procedure was applied in the case of the passive transfer of IgG fraction of polyclonal serum (D, E, F). Error bars indicate SD values. An asterisk indicates a significant ($P < 0,05$) difference by two-tailed Student *t*-test compared to results determined for negative control group (PBS).

negative control groups (Fig. 2B), only 50% of mice succumbed to infection in MAb 499 anti HHV2 treated group of mice while in both AG55+LB66 as well as PBS treated groups of mice more than 60% of the mice died (Fig. 2C). Despite some nonspecific effect was observed for negative MAb 499 treated group, comparison of the AG55+LB66 and PBS treated group clearly shown neglible effect of N terminaly specific MAbs (Fig. 2A–C).

Passive immunization with polyclonal PB1-F2 specific antibodies has no significant effect on the course of infection.

Our next point of interested was whether or not passive immunization with polyclonal PB1-F2 specific antibodies has a similar effect on IAV infection as N-terminus MAbs, or whether it is general property of anti-PB1-F2 antibody response. In these experiments mice were immunized with full length protein PB1-F2-MBP. Sera with anti PB1-F2 antibody titer higher than 1600 (determined by ELISA, Table 1) were pooled and used for purification for passive immunization experiments. As a positive control, IgG purified from serum of PR8 infected mice was used. In negative control the group of mice was passively immunized with IgG purified from sera of mice immunized with protein MBP or PBS. Two hr p.i. mice were infected with PR8 ($1LD_{50}$). The survival rate and body weight changes were monitored daily. In comparison to the negative control groups, lung virus titer twice as low was detected in IgG for anti PB1-F2-MBP and comparable virus titer was detected in PBS control group (Fig. 2D) group 2DPI. Despite decreased viral lung load and equal weight change having been observed (Fig. 2E), 80% of mice immunized with IgG anti PB1-F2-MBP succumbed and 70% of mice in the negative control group immunized with IgG anti MBP succumbed as well (Fig. 2F). In PBS negative control group even 90% of the mice have died. Similarly to passive immunization with N terminally PB1-F2 specific MAbs such immunization with polyclonal PB1-F2 specific antibodies does not significantly affect the survival rate of mice following IAV infection. As

Table 1
PB1-F2 specific antibody titer of individual IMS raised after PB1-F2-MBP immunization. 100 ng of synthetic full length PB1-F2 protein was coated on 96 well microtiter plate and absorbed overnight. Individual IMS/NMS were tested on presence and titer of PB1-F2 specific antibodies. Sera were pooled and used for purification for passive immunization experiments. Sera chosen for IgG purification and passive transfer are indicated with ¤.

IMS	titer IMS anti PB1-F2-MBP
1¤	25,600
2¤	3200
3¤	12,800
4¤	12,800
5¤	6400
6	800
7¤	6400
8¤	51,200
9¤	6400
10¤	3200
11¤	51,200
12	800
13¤	12,800
14¤	6400
15	1600
16¤	6400
17	1600
18	800

described earlier, polyclonal specific antibodies present in serum obtained by immunization with PB1-F2-MBP bind predominantly to the N-terminal part of the molecule. Nevertheless, such serum also contains antibodies directed against C-terminal part of PB1-F2 at a low level. As C-terminal specific MAbs were not available, we decided to study the effect of active immunization using PB1-F2 peptides conjugated with KLH and

DNA immunization with plasmids allowing for expression of different parts of PB1-F2 molecule.

Active immunization revealed the protective potential of C-terminal part of the PB1-F2.

We first immunized a group of mice with two doses of PB1-F2 peptides (N_{3-13}, M_{42-53} or C_{71-83}) conjugated to KLH. The positive control group was immunized with purified PR8 virus IAV and the negative control group with KLH protein. Before infection, specific antibody induction was measured by ELISA; sera obtained by immunization with one peptide bind very well to this peptide but did not cross react with remaining peptides (supplementary Fig. 3A). Mice were infected intranasally with PR8/IAV (1 LD_{50}). The survival rate and body weight changes were monitored daily. As RCA method was capable to detect virus level till 6DPI we had switched to much more sensitive detection of vRNA by RT-PCR. Viral RNA load on 2, 6, 10DPI, body weight changes and survival rate were monitored 14DPI. In comparison to negative control group (KLH) 2DPI, lung vRNA load was somewhat higher in all experimental groups (Fig. 3A) (N_{3-13} orM_{42-53} or C_{71-83}). In the context of the above it was surprising that C_{71-83} peptide immunized group exhibit decreased weight (Fig. 3B) but increased % of survival (Fig. 3C) where 90% of mice survived.

In further experiments we employed DNA vaccination. DNA vaccination mimics natural infection with its complex antigen processing as well as immune response. Mice were i.m. immunized with three doses of 50 μg of pPB1-F2 (1–87), pNter (1–50aa) PB1-F2, pCter (51–87aa). PB1-F2, pHA, pPB1-F2 Stop 3aa and PBS in two week intervals. Ten days post final immunization, blood was collected and serum assayed and the presence of immunogen-specific Abs was confirmed (supplementary Fig. 3B). Stop3aa mutation construct was used as negative control. DNA vaccination with plasmid expressing full length PB1-F2 resulted in a decrease in the virus RNA level in comparison to PBS treated group (Fig. 3D). Immunization with remaining plasmids expressing N-terminal, C-terminal has a similar outcome as pPB1-F2 Stop 3aa DNA vaccination. Despite higher level of viral NS RNA was detected in the pC ter. PB1-F2 vaccinated group of mice on 2DPI and 6DPI in comparison to pPB1-F2 or pN ter. PB1-F2, this group had exhibited the lowest weight decrease and the highest survival. The effect of stop mutant plasmid can be attributed to CpG adjuvant effect

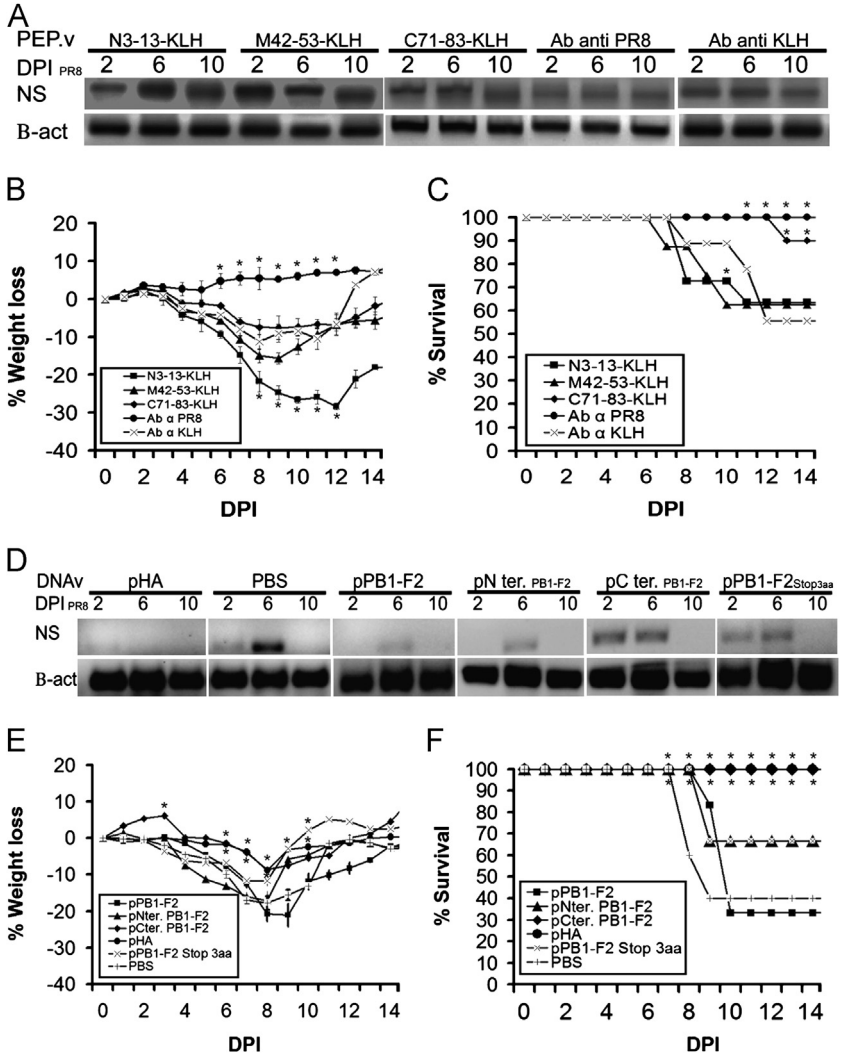

Fig. 3. Effects of active immunization with peptide-KLH and DNAv representing distinct region of PB1-F2 was tested to determine immunological importance of substructural domains of the PB1-F2 throughout the course of IAV infection. In days post infection as indicated, two mice per group were sacrificed, lungs were homogenated in PBS and centrifuged in 4000 RPM for 10 min. Supernatant of the mice from the same group were pooled and used for whole RNA isolation with RNA isolation kit (Ecoli, Slovakia). RNA was reverse transcribed with random hexamer primer and RT-PCR was employed to measure relative levels of influenza NS gene RNA several days post infection. Beta-actin was used as endogenous control in each sample (A, D). Severity of infection was monitored daily. Individual mouse was weighted and body weight change was plotted (B, E). Survival rate for all the experimental group was monitored for two weeks (C, F) and plotted. Error bars indicates SD values. An asterisk indicates a significant ($P < 0,05$) difference by two-tailed Student *t*-test compared to results determined for negative control group (KLH or PBS).

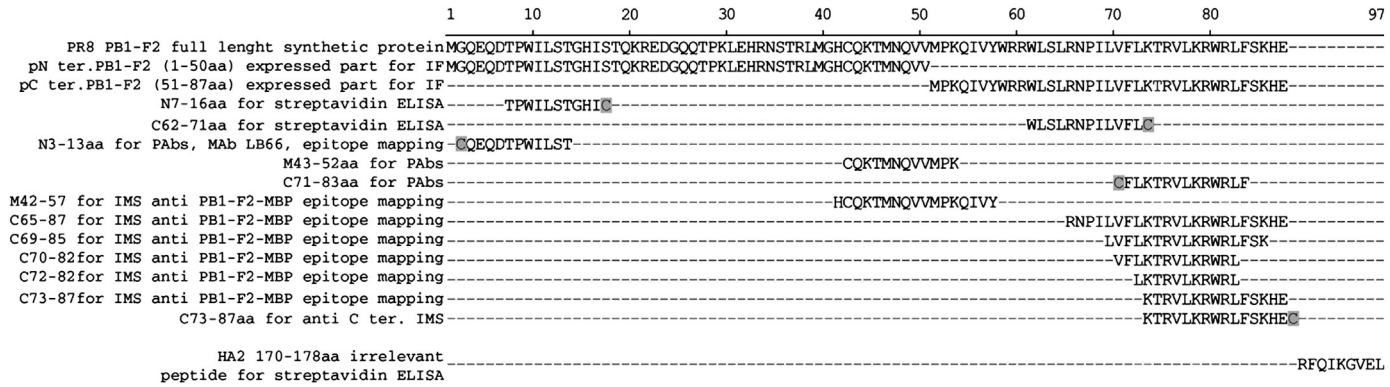

Fig. 4. List of peptides used. Peptide sequences and their location within PB1-F2 molecule are indicated. Moreover application of individual peptides is indicated. All the peptides were designed according to PR8 (H1N1) PB1-F2 amino acid sequence (ACN: ABD77684) except $HA2_{170-178}$ peptide which was from the A/Mississippi/1/1985(H3N2) derived (ACN: AAB69835). Gray rectangles represent synthetically added cystein residue to facilitate peptide conjugation to KLH. Vector NTI Advanced 11.5.0 software package was used to sequence alignment.

(Bode et al., 2011; Smahel et al., 2011). As follows from body weight change and rate of survival, DNA immunization with plasmid expressing C-terminus (51–87aa) induced excellent protection with 100% of survival and minimal weight loss in the indicated sublethal dose of infection $1LD_{50}$ (Fig. 3E, F). The DNA vaccination against IAV elicits humoral as well as cellular immune responses with protective potential (Charo et al., 2004; Choi et al., 2009; Ilyinskii et al., 2008; Shen and Niu, 2012). PB1-F2 specific CTL probably play minor role in comparison to PA or NP specific CTL response in mouse model respectively (La Gruta et al., 2008). Nevertheless in DNA vaccination with pCter (51–87aa) the contribution of CTL response may not be excluded as pCter expresses experimentally proved immunodominant PB1-F2 (62–70aa) MHCI binding peptide (Chen et al., 2001; La Gruta et al., 2008). It follows from active immunization experiments that antibodies against C-terminal part of the PB1-F2 express reasonable protection against IAV infection. As efficient uptake of the C-terminal derived peptide of the PB1-F2 was shown on macrophage cell line J774 and C-terminus is considered to be responsible for the immunopathology of IAV infection (McAuley et al., 2007; McAuley et al., 2010a) antibodies specific to the C-terminal region could inhibit these functions, especially in the later phases of infection due to the cytopathic release of PB1-F2 from infected epithelial cells. Such released PB1-F2 molecules can quickly enter other cells and induce their death due to the presence of C-terminal part. Antibodies against the C-terminal part of PB1-F2 could bind to released PB1-F2 molecules and prevent their entry to other cells.

Conclusion

During IAV infection antibodies against the C-terminal part of PB1-F2 are induced together with antibodies recognizing N-terminal part of PB1-F2. Antibodies recognizing N terminal part of the PB1-F2 have no significant effect whereas antibodies against C terminal part of the PB1-F2 partially protect mice against infection. We assume that if both types of antibodies are present the protective effect of antibodies against the C-terminal part of PB1-F2 is lost. One possible explanation is that antibodies against N-terminal PB1-F2 dominate over antibodies C-terminal part of PB1-F2 during immune response. The biological relevance of anti-PB1-F2 specific antibodies in IAV infections seems to be very complex.

Materials and methods

Virus, cell line and mice: A/PR/8/34 (H1N1) (Kindly provided by Dr. Yewdell, NIH, USA), MDCK and female six week old BALB/c were used in this study. In all experiments presented in this paper, animals were treated according to the European Union standards and the fundamental ethical principles including animal welfare requirements were respected.

Antibodies and antigen preparation:

MAb AG55specific to the N-terminal region of the PB1-F2 preparation has been previously described (Krejnusova et al., 2009). N-terminal specific MAb LB66 was prepared by standard hybridoma technique after immunization of the mice with peptide N_{3-13} (CQEQDTPWILST) conjugated to KLH. KLH-C_{73-87} (KTRVL KRWRLSFKHEC) peptide of the PB1-F2 was used for preparation of the mouse PAbs. Additional peptides M_{42-53} (CQKTMNQVVMPK) and C_{71-83} (CFLKTRVLKRWRLF) were conjugated to KLH via m-maleimidobenzoyl-N-hydoxysuccinimide ester (Thermo Scientific) by the protocol recommended by supplier in order of PAbs induction. Biotin-TPWILSTGHIWEREC$_{7-16}$, Biotin-WLSLRNPILVF-LC$_{62-71}$ and irrelevant peptide HA2 derived RFQIKGVEL$_{170-178}$ used in ELISA were produced by, Metabion, Germany. Synthetic full length protein PB1-F2 derived from PR8 virus was used for PB1-F2 specific antibody level determination (Roder et al., 2008). The remaining peptides corresponding to different regions of the PB1-F2 molecule were kindly provided by Dr. Yewdell (NIH, USA). All the peptides and plasmid coded sequences used in described experiments are summarized in Fig. 4. MBP and fusion protein PB1-F2-MBP were prepared using the pMAL-c2X.MBP Protein Fusion and Purification System (New England Biolabs). Monoclonal and polyclonal antibodies were purified by standard procedure on protein A sepharose collumn.

For PAbs preparation, groups of 18 BALB/c mice were i.p. immunized with three doses of approximately 15 μg PB1-F2-MBP or about 15 μg MBP with complete or incomplete Freund's adjuvant per mouse in three-week intervals. Sera were collected two weeks after last dose. Monoclonal and polyclonal antibodies were purified by standard procedure on protein A sepharose column.

MAb 499 specific to gB-2 of HHV-2 virus was used as negative control, MAb H17L2 specific to HA of PR8, kindly provided by Dr. Gerhard (USA) was used as positive control. MAb 107L (Vareckova et al., 1995) specific to NP of PR8 was used in rapid culture assay (RCA). Irrelevant IMS raised against MHV68 was kindly provided by Dr. Chalupkova from Department Microbiology and Virology of the Faculty of Sciences, Comenius University, Bratislava.

Passive Abs transfer: Groups of 8–16 mice were passively i.v. immunized with purified MAbs: 100/100 μg AG55+LB66, 30 μg H17L2 and 150 μg 499 per mouse. Groups of 16 mice were passively immunized i.v. by PAbs: 160 μg IgG anti PB1-F2-MBP, 60 μg IgG anti PR8 and 150 μg IgG anti MBP. Mice were infected i.n. $1LD_{50}$ of PR8 2 h post receiving antibodies.

Peptide-KLH and pDNA immunization: Groups.of 16 mice were i.p. immunized with two doses of 100 μg N_{3-13} or M_{42-53} or C_{71-83} KLH conjugates with complete or incomplete Freund's adjuvant per mouse in two week intervals. Control groups were immunized with purified virus or KLH (50 μg per mouse). Ten days post the final immunization, blood was collected and serum assayed for the presence of immunogen-specific Abs. For DNA vaccination groups of 14 mice were i.m. immunized with three doses of 50 μg of pPB1-F2, pNter.PB1-F2, pCter.PB1-F2, pHA or pPB1-F2 Stop 3aa or PBS in two week intervals. Ten days after last dose and serum was assayed for presence of specific Abs. Stop3aa mutation construct revealed by sequencing during PB1-F2 cloning was used as negative control.

Infection: Mice were i.n. infected with 1 LD50 of PR8 virus diluted in 40 μl PBS.

RT-PCR: To determine viral RNA, previously published assay was employed (Kosik et al., 2012) and the NS gene was used as a marker (Birch-Machin et al., 1997). Total RNA was extracted from 100 μl of mouse lung homogenate using a Total RNA Isolation Kit (SbsBio), reverse-transcribed using an oligo(T) primer with Mu-MLV reverse transcriptase (Fermentas), and subjected to PCR amplification using the PR8 virus NS gene-specific primers AC: CY035146 (5′-GCTGGAAAGCAGATAGTGGA-3′[forward] and 5′-GCCTGGTCCATTCTGATACA-3′[reverse]). β-actin was used as internal control with the primers AC: NM_007393 (5′-AGGTGACAGCATTGCTTCTG-3′[forward] and Betact Rev 5′-GCTGCCTCAACACCTCAAC-3′[reverse]). The cycling consisted of 95 °C for 5 min, 94 °C for 15 s, 58 °C for 30 s, 35 cycles of 72 °C for 30 s, and 72 °C for 5 min. PCR products were separated by agarose gel electrophoresis and stained with ethidium bromide.

ELISA: Peptides of PB1-F2, PB1-F2-MBP, MBP, synthetic full length PB1-F2 and PR8 purified virus were adsorbed onto wells of microtiter plates (Costar), washed, and saturated with 1% of BSA. Initial 100-fold diluted serum samples were serially diluted and added into the wells. Following incubation and washing, the binding of immunoglobulins to antigens was detected with rabbit anti-mouse IgG conjugated to horseradish peroxidase and 1,2-phenylene-diamine-dihydrochloride at 492 nm (Krejnusova et al., 2009). Anti PB1-F2-MBP serum diluted 200-fold was analyzed at the same conditions. The antibody titer was calculated as the reciprocal of the sample dilution at the point where the titration curve crossed the cutoff line. Cutoff value was determined as 2-fold absorbance measured for negative controls or NMS samples.

Rapid culture assay (RCA): Viral lung titer was measured as described previously (Tkacova et al., 1997). Briefly, 96-well cell culture plates were seeded with 2.5×10^5 MDCK cells per well and incubated at 37 °C overnight. The cells were incubated with aliquots of serial dilutions of mouse lung homogenates (100 μl/well) for 45 min, washed, and exposed to growth medium containing TPCK-trypsin (Sigma) (95 μl/well) for 18 h. The cells were fixed, washed and then treated with the NP-specific MAb 107L, followed by the polyclonal rabbit anti-mouse HRP conjugate, both at 37 °C for 1 h. Finally, the cells were stained with aminoethyl carbazole(Sigma) in dimethylformamide for 30 min. The virus titer was calculated as the reciprocal of the highest sample dilution yielding at least one single stained cell.

Indirect immunofluorescence: MDCK cells were grown on glass cover slips to 60–70% confluence. The cells were transfected with plasmid DNA using Turbofect (Fermentas). The cells were fixed with 3% paraformaldehyde (Sigma) in PBS for 10 mins and permeabilized with 1% Triton X-100 (KochLight) for 60 s. Samples were washed three times with PBS and incubated with 250-fold diluted IMS raised against PB1-F2-MBP for 1 h at room temperature. Subsequently, the washing step was repeated as described previously, and the cells were incubated for 1 h with the 100-fold diluted secondary goat anti mouse FITC conjugated antibody (DAKO). For confirmation of PB1-F2 variants (either full length or N terminal or C terminal part) expression, samples were incubated with AG55 MAb specific to N terminal part of the PB1-F2 or 50-fold diluted IMS anti KLH-PB1-F2 73–87aa for 1 h at room temperature. Samples were washed and incubated 1 h at room temperature with 100-fold diluted goat anti mouse Texas Red conjugated secondary antibody (Sigma Aldrich). After the final wash step, the samples were mounted with DAPI (4′,6-diamino-2-phenylindole) containing mounting medium (Santa Cruz Biotechnologies). Fluorescence was visualized with a confocal microscope LSM Zeiss 510 Meta (Kosik et al., 2012).

Western blotting (WB): Six well tissue culture plates were seeded with MDCK cells. At 60–70% confluence cells were transfected with 4 μg of the different pDNA. 24HPT and 48HPT cells were washed twice with PBS and directly lysed on the plate by 2XSDS lysis buffer and incubated for 5 min at 100 °C. Samples were centrifuged 15 min 14,000 RPM and separated by 15% SDS-polyacrylamide gel electrophoresis (PAGE) under reducing conditions. The proteins were electroblotted onto nitrocellulose membrane (Schleicher and Schuell; 0.45 μm) in 10 mM Tris-glycine buffer with 20% methanol. Blots were blocked overnight at 4 °C in PBS containing 1% BSA, washed twice with PBS. Membrane was cut and strips were incubated with five 1000-fold diluted MAb AC-15 anti β-actin MAb (Sigma-Aldrich) or AG55 MAb (5 μg/ml) or 1000-fold diluted IMS anti PB1-F2-MBP in PBS containing 1% BSA and 0,001% NP-40 for 2 h at RT and washed in PBS. After extensive washing, the strips were incubated for 2 h with Alexa Fluor 790 Goat Anti-Mouse IgG (H+L) (Molecular Probes®) diluted in 1% BSA and 0,001% NP-40 in PBS and washed with 0.001% NP-40 in PBS. Immunoreactive bands were visualized by Odyssey CLx Infrared Imaging System (Li-Cor).

Statistical analysis: Statistical analysis was performed using GraphPad Prism softwareV5.00 (GraphPad Software Inc., San Diego, CA). Unpaired two-tailed Student *t*-test was applied to comparison of experimental groups to negative control groups in individual experiments. The differences were considered statistically significant at $p < 0,05$.

Acknowledgments

This work was supported by grants VEGA 2/0175/09, 2/0085/102/0176/12, 2/0100/13, and 2/0117/11 from the Scientific Grant Agency of the Ministry of Education of the Slovak Republic and Slovak Academy of Sciences. The topic was also supported by Grant no. APVV-0250-10, from the Slovak Research and Development Agency. Appreciably topic was further supported by Eva Varečková (DO7RP-0025-10 from the Slovak Research and Development Agency). We are also thankful to Jack R. Bennink and Jonathan W. Yewdell from the Laboratory of Viral Diseases, National Institute of Allergy and Infectious Diseases, NIH, Bethesda, USA, who kindly provided synthetic peptides, full length protein PB1-F2, pMAL-c2X.MBP. The authors thank Margita Mišovičová for her excellent technical assistance.

Appendix A. Supporting information

Supplementary data associated with this article can be found in the online version at http://dx.doi.org/10.1016/j.virol.2013.08.022.